# Electrical Properties of $Mn_{3-x}Co_xO_4$ ($0 \leq x \leq 3$) Ceramics: An Interesting System for Negative Temperature Coefficient Thermistors

**A. Rousset, C. Tenailleau,* P. Dufour, H. Bordeneuve, I. Pasquet, and S. Guillemet-Fritsch**

*Institut Carnot CIRIMAT, Université Paul Sabatier, UMR CNRS 5085, 118 Route de Narbonne, 31062, Toulouse Cedex 9, France*

**V. Poulain and S. Schuurman**

*Vishay Resistors Belgium, Rue des deux maisons, 37, 1140 Bruxelles, Belgium*

Single-phase spinel manganese cobalt oxides $Mn_{3-x}Co_xO_4$ dense ceramics were prepared for the first time and their structural/electrical property relationships characterized. The electrical properties, that is, the resistivity at 25°C, the energetic constant, and the resistance drift at 125°C, were determined and correlated with the cation distribution. Finally, the electrical characteristics of the $Mn_{3-x}Co_xO_4$ system were compare'd with other important classes of manganese-based spinel oxides, $Mn_{3-x}Ni_xO_4$ and $Mn_{3-x}Cu_xO_4$, already commercialized as negative temperature coefficient (NTC) thermistors. The high values of energetic constant and low resistivities observed in $Mn_{3-x}Co_xO_4$ ceramics present a promising interest for such industrial applications.

## Introduction

The examination of the $Mn_3O_4$–$Co_3O_4$ phase diagram[1] shows that conventional sintering of $Mn_{3-x}Co_xO_4$ ($0 \leq x \leq 3$) powders at $1150 < T < 1300$°C does not easily allow the formation of single-phase ceramics. This characteristic certainly explains the small amount of publications related to the whole $Mn_3O_4$–$Co_3O_4$ system for bulk ceramics, which are rarely proposed for negative temperature coefficient (NTC) thermistor applications, in comparison with $Mn_{3-x}Ni_xO_4$ or $Mn_{3-x}Cu_xO_4$ systems.[2–6] The electrical

*tenailleau@chimie.ups-tlse.fr

resistance of those spinels is highly sensitive to temperature, and makes them useful passive components for temperature regulation and measurement, as well as thermal variation compensators, high frequency power measurements, and fluid (flux or level) measurements. Telecommunications (mobile phones), transports (captors, electronic injection), space, and medicine are among the main application areas of such semiconductors.

The conductivity of these ceramics, generally made of transition metal oxides like spinel manganites $Mn_{3-x}M_xO_4$ (M = Ni, Cu, ...), is due to the presence of donor/acceptor $M^{n+}/M^{(n+1)+}$ couples in the octahedral sites ($Mn^{3+}/Mn^{4+}$ for manganites) that contribute to an electronic exchange by a hopping mechanism according to the Verwey's law.[7] The conduction mechanism is interpreted by the small polaron model[8] and the resistivity ρ can be calculated using the following relationship:

$$\begin{aligned}\rho &= 1/\sigma \\ &= [(\sqrt{2}\cdot d\cdot k\cdot T)/e^2\cdot \nu_o\cdot N\cdot C\cdot(1-C)] \\ &\quad \cdot \exp(E_a/k\cdot T) \\ &= \rho_o\cdot\exp(B/T) \end{aligned} \quad (1)$$

with: σ (S/m) = conductivity

$d$ = shortest donor/acceptor distance in the octahedral sites

$k$ = Boltzmann's constant

$T$ (K) = temperature

e = charge of the electron

$\nu_o$ = frequency of the network vibration $\sim 10^{13}$ $s^{-1}$

$N$ = density of charge carriers $[M^{n+} + M^{(n+1)+}]$

$C$ = cation donors ratio $[M^{n+}]/[M^{n+} + M^{(n+1)+}]$

$1 - C$ = cation acceptors ratio $[M^{(n+1)+}]/[M^{n+} + M^{(n+1)+}]$

$NC(1 - C) = [M^{n+}][M^{(n+1)+}]/[M^{n+} + M^{(n+1)+}]$

$E_a$ = activation energy for the hopping mechanism

$B = E_a/k$ = energy constant or thermal sensitivity factor for a NTC thermistor

This relationship must be rigorously applied to single crystals. Structural ordering and screening effects due to cations in octahedral sites that do not participate to the hopping mechanism can also occur in such materials. Therefore, differences in resistivity between experimental and calculated values can be noticed. However, it is usually possible to confirm or exclude a cation distribution after structural and/or spectroscopic determinations based on the resistivity variations with composition.[2,5,9,10] As a consequence, the electrical characteristics are essential for the structural comprehension of oxides and applications for NTC thermistors. The example of the $MnCo_2O_4$ compound is significant. Its cation distribution is usually described by $Co^{2+}[Co^{III}Mn^{3+}]O_4^{2-}$ with $Co^{III}$ being a trivalent cobalt ion in a low spin state, that is, $t_{2g}^6e_g^0$.[11–13] But the high conductivity value measured for $MnCo_2O_4$ cannot be explained by this distribution with the absence of donor/acceptor couples in the octahedral sites.

Recently, we have been able to obtain single-phase ceramics of $Mn_{3-x}Co_xO_4$ over the whole solid-solution range using appropriate thermal treatments with conventional sintering technique and spark plasma sintering (SPS) method.[14] The SPS technique, which allows the formation of ceramics with very high densities while sintering temperature, time, and grain size are smaller than for conventional sintering method, was essentially used for $x \geq 1.78$ to obtain pure phases. The sample reactivity studies with oxygen for Co-rich phases ($2 < x < 3$)[15] and neutron diffraction measurements have led us to suggest a substitution mechanism of manganese by cobalt and an unusual cation distribution in the octahedral environments of the spinel structure for the most controversial sample compositions, that is, for $1 \leq x \leq 3$.[16] Thus, it is interesting to study in more details the influence of the substitution of Mn by Co, with similar cation radii and various oxidation and spin states, over the ceramic structural, magnetic, and electrical properties.

In this article, we first present the electrical properties of the most interesting $Mn_{3-x}Co_xO_4$ ($0 < x < 3$) ceramics for NTC thermistors applications. Then, we study their (micro)structural and electrical properties relationships. We particularly focus on the correlation between the resistivity variation and the complex cation distribution with the presence of $Mn^{2+}$, $Mn^{3+}$, $Mn^{4+}$, $Co^{2+}$ and $Co^{III}$ (the latter cation being in a "low spin" state). Finally, the electrical characteristics of $Mn_{3-x}Co_xO_4$ are compared with $Mn_{3-x}Ni_xO_4$ and $Mn_{3-x}Cu_xO_4$, the latter materials being intensively used as NTC thermistors.

## Experimental Procedure

### *Preparation*

The methods of preparation and (micro)structural characterization of sample powders and ceramics have been detailed in previous works.[15,16] Briefly, stoichiometric proportions of metal nitrate salts were mixed with ammonium oxalate, precipitated in ethanol, filtered,

washed and dried, and decomposed at 800°C for 4 h in air. The formation of single-phase ceramics (without cracks) over the whole solid solution range necessitates the transformation of the resulting sample powders by two sintering processes[1]: (i) for $x < 1.78$, by conventional sintering in air, between 1160°C and 1300°C followed by a calcination for 1 h at 900°C and quenching in air (see Table I); (ii) for $x \geq 1.78$, to avoid the formation of a mixture of a spinel phase with CoO, the spark plasma sintering (SPS) technique was used. Dense single-phase ceramics were thus obtained in a few minutes only at lower temperatures (700–750°C).

### *Characterization*

Structural characterizations were made using the X-ray and neutron diffraction techniques.[14,16] Room temperature X-ray diffraction (XRD) measurements were systematically performed on powders and sintered ceramics using a Bruker D4 powder diffractometer ($CuK\alpha_{1,2}$ radiation, 40 kV and 40 mA). Neutron diffraction data were obtained at room temperature on Polaris at the Rutherford Appleton Laboratory, Didcot, U.K., and on the Super D2B instrument available at the Institut Laue Langevin, Grenoble, France. Around 0.3–3.5 g of ceramics was ground into powders before insertion into vanadium cylinders measurements. The particle size and morphology of the products were analyzed using a field electron gun scanning electron microscope (JEOL 6700F, Tokyo, Japan) and with a bright-field transmission electron microscopy (TEM, JEOL, JEM 2010).

### *Electrical Properties Measurements*

To measure the electrical resistivity of the ceramics, the electrodes have to be placed on the two faces of the chip. Two different methods of metallization have been used. The classic method, used in industry and called "serigraphy," consists of depositing a silver mixture on the ceramic. An annealing at 850°C followed by a fast cooling (255°C/min) is necessary to produce the mechanical adherence of the silver paste on both faces of the chip. In the second method, the faces of the ceramics were covered with a thin film of gold, obtained by evaporation under vacuum (10 mbar). In this case, no further heat treatment is needed after the sintering process. Resistance measurements were taken at 25.00 ± 0.05°C using a Philips PM2525 multimeter (Eindhoven, The Netherlands).

The resistivity values ρ were then deduced from the resistance values using the simple relation: $\rho = R \times S/e$, where S and e are the surface and thickness of the ceramic, respectively.

The energy constant $B$ is obtained after measurement of resistances $R_1$ and $R_2$ at two different temperatures $T_1$ and $T_2$ (in our case 298 and 358 K, respectively), when the sample resistance (or resistivity) has a strong temperature dependence, using the following relation:

$$B = \frac{T_1 \cdot T_2}{T_2 - T_1} \cdot \ln\left(\frac{R_1}{R_2}\right) \qquad (2)$$

The electrical stability under thermal constraint was determined based on the resistance variation $\Delta R/R$ of ceramics maintained at 125°C in air for a maximum time of 500 h.

## Results

### *Structure and Microstructure*

Ceramic oxide spinels are tetragonal for $x < 1.78$ and cubic for further $x$ values. X-ray diffraction patterns recorded at 298 K of $Mn_{3-x}Co_xO_4$ ceramics prepared by the conventional method before the structural transition and by the SPS technique for further $x$ values are shown in Fig. 1. The sintering process, conventional or SPS, has little influence on the crystal cell parameter values. For instance, when $x = 1.54$ (tetragonal phase), $a = 8.2237(3)$ Å and $c = 8.6041(3)$ Å using the conventional method while $a = 8.2250(2)$ Å and $c = 8.6020(4)$ Å with the SPS technique. When $x = 1.78$ (cubic phase), $a = 8.3183(4)$ and $8.3130(1)$ Å for the conventional and SPS sintering processes, respectively. The cell variations are identical for single-phase ceramics and powders of the same compositions.[16] This observation is compatible with a substitution mechanism of manganese by cobalt that can be summarized as follows, $Mn_3O_4$ being taken as the basic matrix:

$$\text{For } 0 \leq x \leq 1 : Mn^{2+}[Mn^{3+}{}_2]O^{2-}{}_4 \rightarrow Co^{2+}{}_xMn^{2+}{}_{1-x}[Mn^{3+}{}_2]O^{2-}{}_4 \rightarrow Co^{2+}[Mn^{3+}{}_2]O^{2-}{}_4$$

$$\text{For } 1 \leq x \leq 3 (0 < y < 0.40) : Co^{2+}[Mn^{3+}{}_2]O^{2-}{}_4 \rightarrow Co^{2+}[Co^{2+}{}_yCo^{III}{}_{x-y-1}Mn^{3+}{}_{3-x-y}Mn^{4+}{}_y]O^{2-}{}_4 \rightarrow Co^{2+}[Co^{III}{}_2]O^{2-}{}_4$$

**Table I. Experimental Sintering Conditions**

| | Conventional Sintering | | | | | SPS† | | | | |
|---|---|---|---|---|---|---|---|---|---|---|
| x | Sintering *T* for 8 h (°C) | Dwell *T* for 1 h (°C) | Quenching *T* (°C) | Type of phase* | Densification (%) | Sintering *T* 50°/min (°C) | Dwell time (min) | Pressure (MPa) | Type of phase* | Densification (%) |
| 0 | 1300 | 1200 | 1100 | TS | 87 | | | | | |
| 0.58 | 1300 | 1100 | 1100 | TS | 95 | | | | | |
| 0.98 | 1280 | 900 | 900 | TS | 94 | | | | | |
| 1.27 | 1180 | 900 | 900 | TS | 93 | | | | | |
| 1.54 | 1180 | 900 | 900 | TS | 93 | 750 | 20 | 50 | TS | 95 |
| 1.66 | 1160 | 900 | 900 | TS | 94 | | | | | |
| 1.78 | 1160 | Cooling at 10°C/h | | CS | 94 | 750 | 20 | 50 | CS | 95 |
| 1.99 | | | | | | 750 | 20 | 50 | CS | 95 |
| 2.22 | | | | | | 700 | 20 | 50 | CS | 97 |
| 2.39 | | | | | | 700 | 20 | 50 | CS | 97 |
| 2.60 | | | | | | 700 | 20 | 50 | CS | 97 |
| 2.72 | | | | | | 700 | 20 | 50 | CS | 96 |
| 2.77 | | | | | | 700 | 20 | 50 | CS | 96 |
| 2.93 | | | | | | 700 | 20 | 50 | CS | 96 |
| 3 | | | | | | 700 | 20 | 50 | CS | 92 |

*TS and CS: tetragonal and cubic spinel phases, respectively.
†Nonlinear cooling rate (~5 min).

In the second composition range, the cation distributions showed for the first time in oxide spinel ceramics a double mixed valency for manganese ($Mn^{3+}/Mn^{4+}$) and cobalt ($Co^{2+}/Co^{III}$). These distributions were established after a detailed examination of the neutron diffraction patterns, using the bond valence sum (BVS) calculations and also by using Poix's method.[16] Besides, these results are in strong agreement with the study of the oxidation–reduction mechanisms obtained by thermal analysis of cobalt-rich powders ($2 < x \leq 3$).[15]

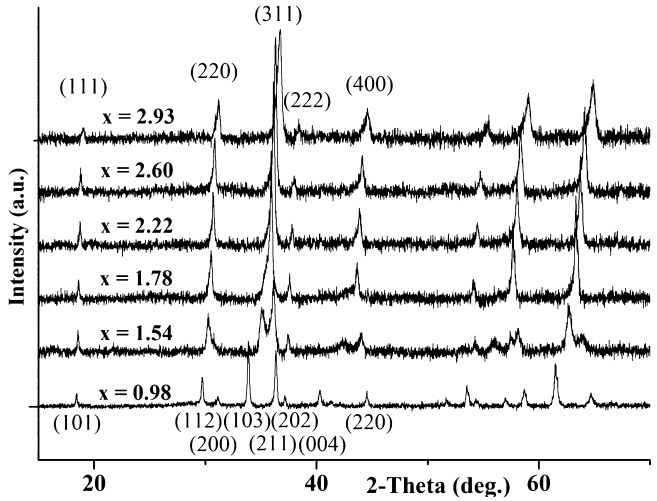


*Fig. 1. Room temperature X-ray diffraction patterns of $Mn_{3-x}Co_xO_4$ ceramics.*

The SEM images of ceramics made by conventional sintering methods showed a large dispersion of the grain sizes varying from a few micrometers to a dozen of microns with a porosity that is mainly closed (Fig. 2 and Ref. 16). On the contrary, ceramics obtained by the SPS technique are constituted by much smaller grains, generally submicronics (0.1–0.7 μm) and more homogeneous in size. No porosity was observed in the volumes of ceramics. The densification is very high, and the density of grain boundaries that can influence the electrical properties is very important.

The microstructural examination by TEM of the oxide spinels showed that for $x < 1.78$, ceramics usually exhibit lamellas of variable thickness depending upon the sample composition, quenching temperature, and sintering technique. These lamellas are twins related to the cubic-tetragonal phase transformation occurring upon cooling (N. El Horr, S. Guillemet-Fritsch, A. Rousset, and C. Tenailleau, unpublished data). This type of defects was already observed in $Mn_3O_4$, $Mn_{3-x}Ni_xO_4$ and $Mn_{3-x-y}Ni_xCo_yO_4$ systems.[17,18] However, ceramics of cubic symmetry ($x \geq 1.78$) present no defects (no

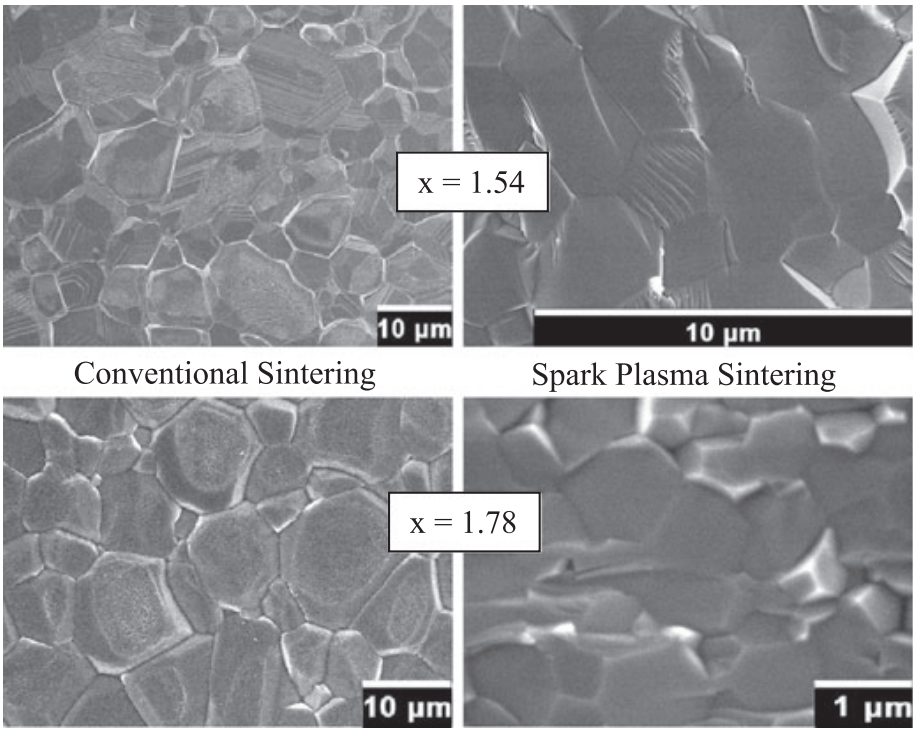


*Fig. 2. SEM images of single-phase ceramics of $Mn_{1,46}Co_{1,54}O_4$ (tetragonal) and $Mn_{1,22}Co_{1,78}O_4$ (cubic) composition sintered in a conventional way and by spark plasma sintering.*

twins, in particular) using either the conventional or sintering technique. This can be explained by the absence of tetragonal-cubic phase transformation upon cooling as can be seen in the phase diagram.[1]

### *Electrical Properties*

*Resistivity ρ: Influence of the Metallization:* The ceramic disks were metallized on both faces either by evaporation under vacuum of gold at room temperature or by serigraphy with a silver print heated up at 700°C in air. In the latter case, a mixture of two tetragonal phases is observed for manganese-rich spinel oxides ($0 < x < 1.54$) due to thermal treatment, according to the phase diagram, and the resistivity values then become very high. But this result cannot be representative of the original composition. Therefore, for those compositions ($0 < x < 1.54$), only the first technique of metal deposition could be used (Fig. 3). For cobalt-rich samples ($1.54 \leq x \leq 3$), the serigraphy post-thermal treatment preserves the single-phase state and both techniques of metallization gave very similar results (insert in Fig. 3). The small differences can be attributed to the thermal treatment at 700°C for the serigraphy, which can modify the cation positions and/or their oxidation states in the spinel crystal structure.

*Influence of the Sintering Process:* Both conventional and SPS sintering techniques allow the preparation of single-phase ceramics that present identical resistivity values (ρ = 475(5) and 466(10) Ω·cm for $x = 1.54$ at 25°C, and ρ = 387(7) and 380(8) Ω·cm for $x = 1.78$). This is an interesting result for the study of the electrical properties. Besides, knowing the differences in microstructure due to the two sintering techniques, the grain size and the grain boundary density have no effect over the resistivity values, in agreement with previous reports on nickel manganites, for instance.[19] For $0 < x < 3$, sample densities are very close (between 93% and 97%) and do not seem to have a strong influence on the electrical resistivity values.

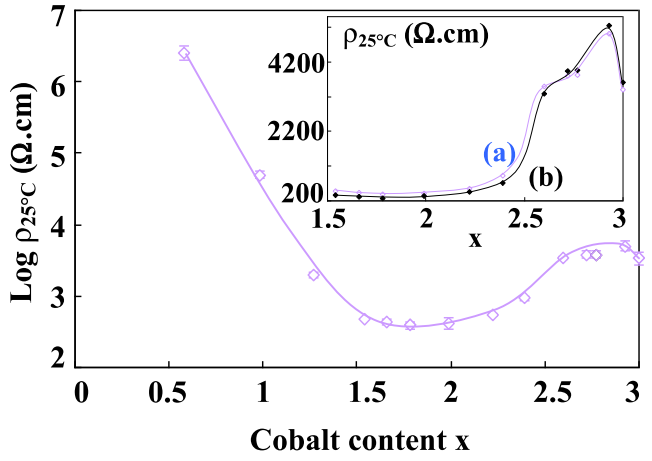


*Fig. 3. Resistivity $\rho_{25°C}$ for ceramics $Mn_{3-x}Co_xO_4$ ceramics at room temperature, after metallization by cathode pulverization, as a function of composition. Variations in the resistivity $\rho_{25°C}$ as a function of cobalt content ($Mn_{3-x}Co_xO_4$ ceramics with $1.54 < x < 3$) after cathode pulverization (a) and serigraphy (b) are shown in insert.*

*Influence of the Composition:* The resistivity variation for $Mn_{3-x}Co_xO_4$ ($0 < x < 3$) at 298 K, represented in Fig. 3, shows two main features. First, a big drop in resistivity is noticed when manganese is substituted by cobalt; and second, a small variation in resistivity appears for $1.5 < x < 2.3$, which is located in the composition area of the tetragonal to cubic phase transformation ($x \sim 1.78$) and where a difference between twinned samples and others with no more planar defects was observed. As a consequence, these phenomena have almost no influence on the resistivity values. This latter result is also essential from an industrial point of view, especially for the fabrication of NTC thermistors as it will be discussed later on. We will try to connect this resistivity behavior to the cation distribution in the spinel network.

*Influence of the Temperature:* Resistivity measurements were performed between 25°C and 150°C, where only samples prepared by serigraphy ($x \geq 1.54$) with no degradation of the metal layer could be studied. The linear curves of ln(ρ) as a function of the inverse of temperature are characteristics of a semiconductor behavior,[14] following the law:

$$\rho = \rho_0 \cdot \exp\left(\frac{E_a}{k \cdot T}\right) = \rho_0 \cdot \exp\left(\frac{B}{T}\right)$$

already encountered in many metal transition manganite spinels.[6,7,20] Thermoelectric power measurements confirmed that these semiconductors were of *p*-type.[21]

### *Energetic Constant B*

The energetic constant, usually noted *B*, is directly related to the activation energy $E_a$ by the relationship

$B = E_a/k$, with $k$ the Boltzmann's constant. From the slopes of the linear variations observed for $\ln\rho = f(1/T)$, it is possible to calculate the energetic constant value, which is interesting for NTC applications since it shows the thermal sensitivity of a material resistance. The variations of $B$ and ρ with sample composition are parallel for $1.5 < x < 2.6$ (Fig. 4) as it is usually observed in manganites used as NTC thermistors. The corresponding activation energy of ~0.36 eV is close to the value reported elsewhere for $Mn_{3-x}Ni_xO_4$ and $Mn_{3-x-y}Ni_xCo_yO_4$ systems.[3,7]

But, for further $x$ values ($x \geq 2.60$), ρ and B vary in an opposite way. The activation energy decreases down to ~0.25 eV, which is the same value found for $Co_3O_4$. There are only a few reports about the activation energies corresponding to the hopping mechanism between divalent and trivalent cobalt ions. The same value of 0.25 eV was already given for $Co_3O_4$ ceramics[22] while activation energies close to 0.50 eV were also reported.[23] It seems that the activation energy, like the resistivity, strongly depends upon the sample preparation method and the sintering conditions that determine the oxygen stoichiometry and spinel inversion ratio.

### *Aging ($\Delta R/R = f(T)$)*

Under thermal constraint in air (at 125°C in the present case), a ceramic undergoes a more or less important variation of its resistivity value as a function of time, that is called aging.[7] Variations of a few tenth of percent appear in copper manganites, for instance.[19,24] This aging phenomenon is prejudicial for the applications. Our previous studies showed a relationship between such resistivity variations and cation distribution modifications (back to the thermodynamic equilibrium state) and/or by the oxidation of some cations.[25–27] This information was useful for the limitation or cancellation of material aging.[3,28,29]

Figure 5 shows the aging phenomenon evidenced for the $Mn_{0.07}Co_{2.93}O_4$ ceramic. The influence of composition on $\Delta R/R$ is shown in Fig. 6. The variations in $\Delta R/R$ and the resistivity with $x$ after 500 h in air are similar. In particular, when the resistivity value is quite stable with the composition ($1.5 < x < 2.3$), only a very small $\Delta R/R$ change (by 0.1%) is noted. These ceramics are thus not very sensitive to the migration and the oxidation of cations in this composition range, which confirms their interesting properties for NTC thermistor applications.

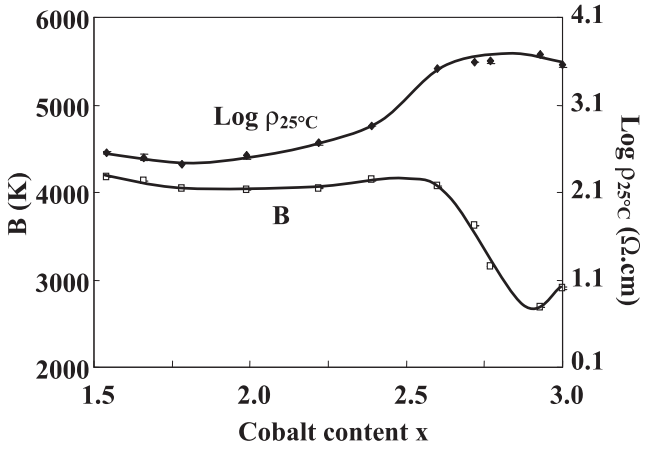


*Fig. 4. Resistivity $\rho_{25°C}$ and the energetic constant B for $Mn_{3-x}Co_xO_4$ ($1.54 \leq x \leq 3$) ceramics metallized by serigraphy as a function of cobalt content.*

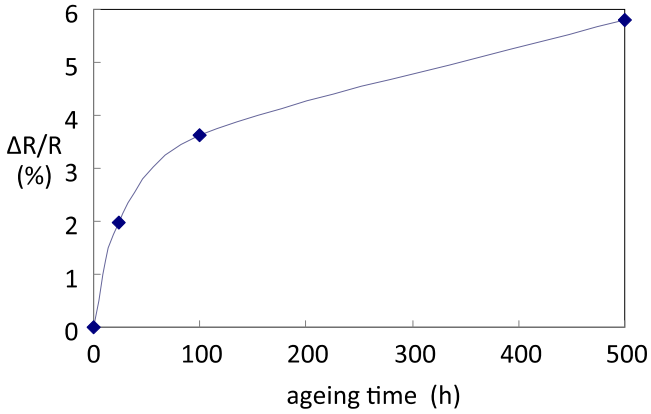


*Fig. 5. Resistance drift $\Delta R/R$ as a function of time, for the ceramic of composition $Mn_{0.07}Co_{2.93}O_4$ measured at 125°C in air.*

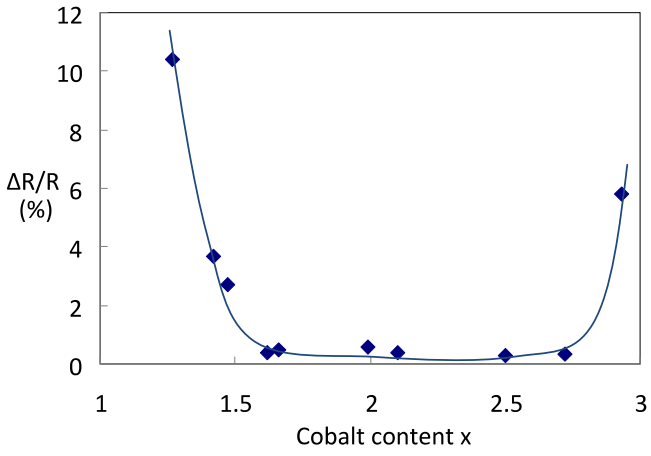


*Fig. 6. Resistance drift $\Delta R/R$ ($t = 500$ h) as a function of cobalt content.*

## Discussion

From these results, it is possible to give a coherent interpretation of the resistivity variation as a function of composition:

For $x \leq 1$, that is, for the Mn-rich spinel domain, the substitution takes place on the tetrahedral sites with $Mn^{2+}$ being replaced by $Co^{2+}$. The corresponding distribution is $Co^{2+}{}_xMn^{2+}{}_{1-x}[Mn^{3+}{}_2]O^{2-}{}_4$ and all samples should be theoretically insulating, just like $Mn_3O_4$ with $Mn^{2+}[Mn^{3+}{}_2]O^{2-}{}_4$ composition. The resistivity values are indeed usually very high, but can vary with the cobalt content. The drop in resistivity observed can be related to the quenching stage that is necessary to obtain single-phase ceramics (Fig. 3). These samples are thus out of their thermodynamic equilibrium state. At high temperature (900–1300°C), the $Co^{2+}$ ions on tetrahedral sites move toward the octahedral sites, thus creating $Mn^{3+}/Mn^{4+}$ couples according to the following process:

$$2Mn^{3+}{}_{oh} \rightarrow Co^{2+}{}_{oh} + Mn^{4+}{}_{oh}$$

This configuration is fixed by the quenching step and the drop in resistivity observed can be explained by the presence of these $Mn^{3+}/Mn^{4+}$ couples. The cell parameters decrease also contributes to the lowering of the resistivity value through the shortening of the cation distances.

For $1 < x < 3$, that is, in the domain where all tetrahedral sites are filled up with $Co^{2+}$ ions, the substitution takes place for the $Mn^{3+}$ ions in octahedral sites. Many authors agree on the fact that the $Mn^{3+}$ ions are replaced by $Co^{III}$ ions according to the $Co^{2+}[Mn^{3+}{}_{2-y}Co^{III}{}_y]O^{2-}{}_4$ $(0 < y < 2;\ y = x - 1)$ model.[11–13] This distribution, characterized by a lack of mixed valency on the octahedral sites, drives to insulating phases whatever the composition is. This hypothesis is in complete disagreement with experimental results, in particular, for the resistivity variation with $x$ (see Fig. 3). The substitution of $Mn^{3+}$ ions by $Co^{2+}$ and $Mn^{4+}$ ions according to the transformation schematic $2Mn^{3+}{}_{oh} \rightarrow Co^{2+}{}_{oh} + Mn^{4+}{}_{oh}$, with the creation of $Mn^{3+}/Mn^{4+}$ couples, was also considered in the past [30,31], but the $Co^{2+}[Co^{2+}{}_yMn^{3+}{}_{2-2y}Mn^{4+}{}_y]O^{2-}{}_4$ model, with $0 < y < 1$ and $y = x - 1$, gives a $y$ value of 1. Therefore, $MnCo_2O_4$ should be an insulator, in contradiction with the experiments that showed a maximum of conductivity around this composition (see Fig. 3). In addition, this model cannot be used for further $y$ values, beyond $MnCo_2O_4$.

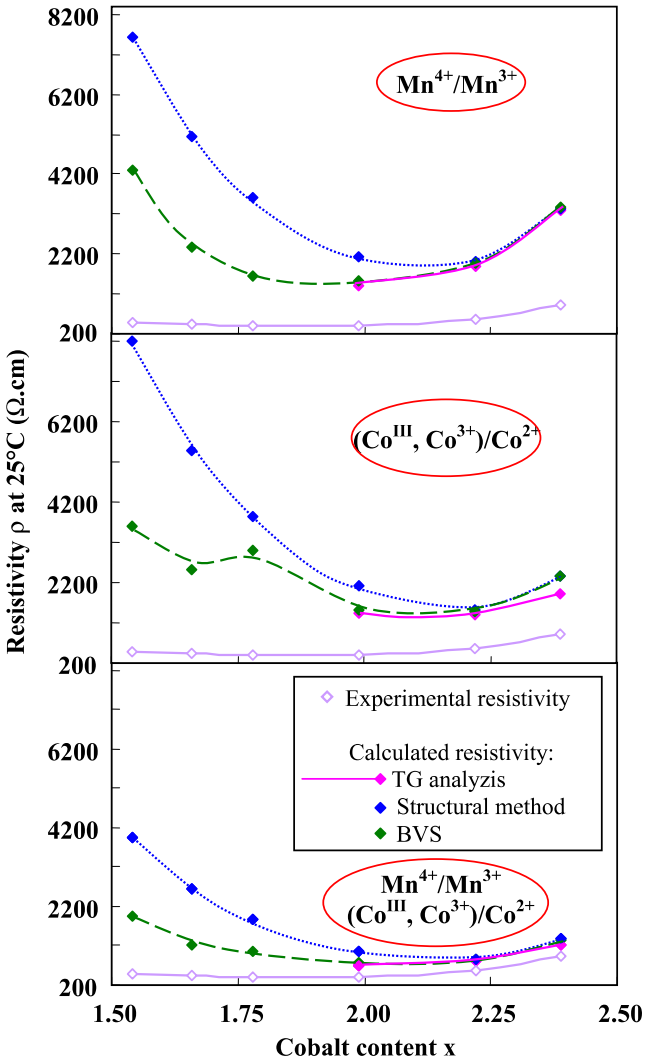


*Fig. 7. Measured and theoretical resistivities as a function of cobalt content in ceramics of composition $Mn_{3-x}Co_xO_4$ $(1.54 \leq x \leq 2.39)$ by considering the cation distributions determined by structural or Poix's method, BVS calculations, and TG analysis (here from $x \geq 2$ only, where the two steps of oxidation–reduction could be identified, see[15]), with different options of cation couples that can participate in the hopping mechanism.*

If we now consider the distribution determined in our studies, that is:

$$Co^{2+}[Mn^{3+}{}_{3-x-y}Mn^{4+}{}_yCo^{2+}{}_yCo^{III}{}_{x-y-1}]O^{2-}{}_4$$
$$(1 < x < 3; 0 < y\,0.40),$$

semiconducting materials with mixed valencies can then be defined, in agreement with experimental results (Fig. 7). Besides, for equivalent concentrations of manganese and

cobalt in octahedral sites, that is, for $x = 2$, the probability of electronic exchange is the highest and the resistivity is the lowest. In addition, if $Mn^{3+}/Mn^{4+}$ couples are predominant for Mn-rich phases ($1 < x < 2$), it appears that $Co^{2+}/Co^{III}$ couples have a donor/acceptor behavior for Co-rich phases ($2 < x < 3$). This is confirmed by resistivity calculations based on the Eq. (1). From the experimental values of the cell parameters, activation energies, and cation distributions, the resistivity values can be calculated by considering either the contribution of $Mn^{3+}/Mn^{4+}$ couples, or $Co^{2+}/Co^{III}$ couples, or both manganese and cobalt couples.[6,15,16] The best agreement between the experimental and calculated resistivity variations with composition is obtained when considering the latter solution, that is, both couples participating in the hopping mechanism. The constant value of resistivity, particularly interesting for NTC thermistors applications as mentioned earlier, can thus be readily explained by the presence of a double mixed valency.

For $x > 2.30$, the resistivity logically increases with composition, which is due to the decrease in active couple numbers.[16] But the value of the resistivity remains largely below the one observed for the Mn-rich phases because it is accompanied by a strong decrease of the activation energy, especially for $x > 2.60$. This opposite variation in the activation energy and resistivity, rather exceptional for NTC materials, can be interpreted with the Eq. (1) only if a small proportion of donor/acceptor couples, especially cobalt (~ a few per cents), is present on the octahedral sites. In fact, it is probably the $Co^{3+}/Co^{2+}$ couples (high spin $Co^{3+}$ with $t^4_{2g}e^2_g$ orbital occupancies) for which the activation energy is lower than for $Co^{III}/Co^{2+}$ couples that contribute to the hopping mechanism. The presence of $Co^{3+}$ and $Co^{III}$ ions has already been mentioned by O'Neil for $Co_3O_4$ and could be induced by the SPS sintering conditions.[31]

We finally performed a comparison between the present system, $Mn_{3-x}Co_xO_4$, and other manganese-based spinel oxides, essentially $Mn_{3-x}Ni_xO_4$ and $Mn_{3-x}Cu_xO_4$, which were largely studied and are used for industrial purposes, in particular NTC thermistors.[3,5,24] Two main factors, the resistivity ρ and the energetic constant *B*, are essential to choose the right system for industrial component. The appropriate domains of composition usually correspond to the smallest variation of resistivity to guarantee better reproducibility and thermal stability.[28] The electrical characteristics of all three systems are shown in Fig. 8. For the Mn-Co system, the (ρ,*B*) couple variation is different from those obtained for the Mn–Ni and Mn–Cu systems. High values of energy constant or sensitivity can be reached for rather small resistivities. The Mn–Cu system exhibits small resistivity values with low sensitivity. For the Mn–Ni system, the sensitivity is slightly smaller than for the Mn–Co system, but the resistivity is still largely more important. This interesting result reinforces the explanation of the conduction mechanism given earlier. Indeed, if the $Mn^{3+}/Mn^{4+}$ couples only participate in the hopping process for nickel (or cobalt) manganites, the minimum of resistivity (with $[Mn^{3+}] = [Mn^{4+}]$) for $Mn^{2+}[Mn^{2+}_{2/3}Mn^{4+}_{2/3}Ni^{2+}_{2/3}]O^{2-}_4$ should be largely smaller than for $Co^{2+}[Mn^{3+}_{0.60}Mn^{4+}_{0.40}Co^{2+}_{0.40}Co^{III}_{0.60}]O^{2-}_4$, with $1/(NC(1 - C)) = 3$ and 4.2 for Ni and Co, respectively. The opposite observation tends to show that both $Mn^{3+}/Mn^{4+}$ and $Co^{2+}/Co^{III}$ couples contribute to the hopping mechanism. The Mn–Co system thus allows a new sets of (ρ,*B*) characteristics to be reached with promising applications for apparatus that require the

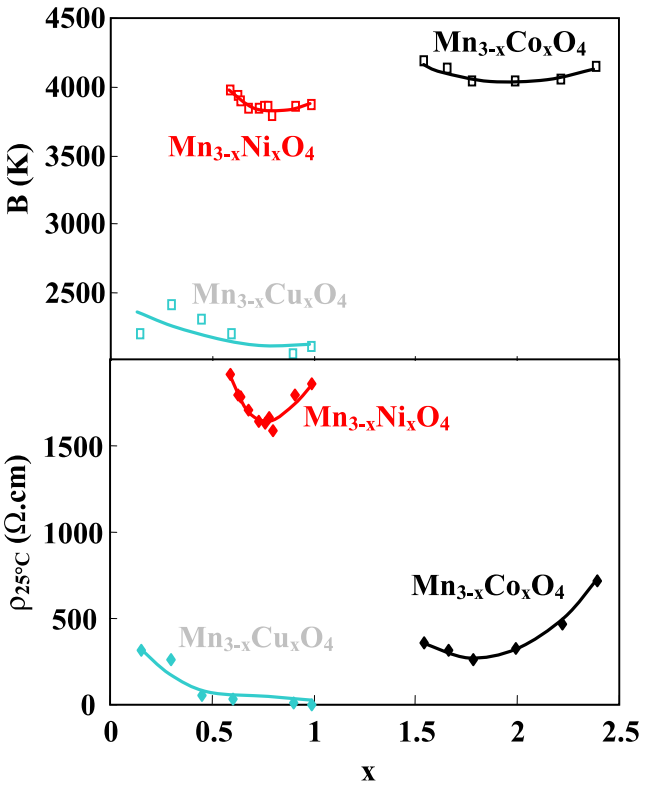


*Fig. 8. Resistivity $\rho_{25°C}$ and energetic constant B as a function of the substitution content in the systems $Mn_{3-x}Ni_xO_4$, $Mn_{3-x}Cu_xO_4$ and $Mn_{3-x}Co_xO_4$.*

detection and measurement of small temperature variation. This system could also be used as a "matrix" for partial substitution of cobalt by nickel and/or copper to enlarge the domain of ($\rho$,$B$) couples. The knowledge of the fine structure of our $Mn_{3-x}Co_xO_4$ ceramics will enhance the control and understanding of such ternary or quaternary complex systems.

The opposite variations in the resistivity and energy constant for the cobalt-rich phases will also require further investigations.

## Conclusions

The electrical properties of $Mn_{3-x}Co_xO_4$ single-phase dense ceramics, with $0 < x < 3$, were established. Their preparation involved the conventional ($0 < x \leq 2$) and SPS ($2 \leq x \leq 3$) sintering processes to avoid the presence of additional phase such as CoO, which can disturb the physical and chemical properties.

$Mn_{3-x}Co_xO_4$ phases are usually $p$-type semiconductors with a conduction mechanism driven by the hopping of small polarons thermally activated between $Mn^{3+}/Mn^{4+}$ and $Co^{2+}/Co^{III}$ ions. Beyond $x = 1$, the presence of this double mixed valency on the octahedral sites of the spinel crystal structure, previously determined by XRD, neutrons and BVS calculations, and confirmed by TG analysis, is in good agreement with the resistivity variation as a function of composition. This configuration can explain the relatively low resistivity values (300–400 Ω·cm) obtained for a large composition range ($1.5 < x < 2.2$). In this case, the resistivity seems rather independent of the cobalt content, sintering condition, thermal treatment, tetragonal to cubic phase transformation, and the presence or not of twins. The presence of this stable domain of resistivity is definitely interesting for the future use of NTC thermistors with reliable and reproducible properties. Thanks to high values of energetic constant ($B >$ 4000 K) associated with rather low resistivities, the Mn–Co system also presents different but complementary characteristics to those of the Mn–Ni and Mn–Cu systems for NTC thermistor applications.

## Acknowledgments

We thank the Vishay company and French CNRS for their financial support.

## References

1. E. Aukrust and A. Muan, "Thermodynamic Properties of Solid Solutions with Spinel Type Structure. The System $Co_3O_4$-$Mn_3O_4$," *Trans. Metal. Soc. Aime*, 230 378–382 (1960).
2. R. Legros, R. Metz, and A. Rousset, "Structural Properties of Nickel Manganite $Ni_xMn_{3-x}O_4$," *J. Mat. Sci.*, 25 4410–4414 (1990).
3. S. Fritsch, *et al.* "Correlation Between the Structure, the Microstructure and the Electrical Properties of Nickel Manganite NTC Thermistors," *Sol. St. Ionics*, 109 229–237 (1998).
4. B. Gilllot, M. Kharroubi, R. Metz, R. Legros, and A. Rousset, "Electrical Properties and Cationic Distribution in Cubic Nickel Manganite Spinels $Ni_xMn_{3-x}O_4$," *Solid State Ionics*, 44 275–280 (1991).
5. R. Metz, J. P. Caffin, R. Legros, and A. Rousset, "The Preparation, Characterization and Electrical Properties of Copper Manganite Spinels $Cu_xMn_{3-x}O_4$," *J. Mat. Sci.*, 24 83–87 (1989).
6. B. Gillot, R. Legros, R. Metz, and A. Rousset, "Electrical Conductivity of Copper and Nickel Manganites in Relation with the Simultaneous Presence of $Mn^{3+}$ and $Mn^{4+}$ Ions on Octahedral Sites of the Spinel Structure," *Solid State Ionics*, 51 7–9 (1992).
7. E. J. W. Verwey, P. B. Braun, E. W. Gorter, E. C. Romeijn, and J. H. Van Sauten, "Die Verteilung der Metallionen im Spinellgitter und deren Einfluss auf die physikalischen Eigenschaften," *Z. Phys. Chem.*, 198 6–22 (1951).
8. E. D. Macklen, *Thermistors*, Electrochemical Publications, Azyr Scotland, 1979.
9. R. Legros, R. Metz, and A. Rousset, "The Preparation, Characterization and Electrical Properties of Electroceramics Made of Copper Cobalt Manganite Spinel $Mn_{2.6-x}Co_{0.4}Cu_xO_4$," *J. Eur. Ceram. Soc.*, 15 463–468 (1995).
10. T. Battault, R. Legros, and A. Rousset, "Structural and Electrical Properties of Iron Manganite Spinels in Relation with Cationic Distribution," *J. Eur. Ceram. Soc.*, 15 1141–1147 (1995).
11. B. Boucher, R. Buhl, R. Di Bella, and M. Perrin, "Etude par des mesures de diffraction de neutrons et de magnétisme des propriétés cristallines et magnétiques de composés cubiques spinelles $Co_{3-x}Mn_xO_4$ ($0.6 \leq x \leq 1.2$)," *J. de Physique*, 31 113–119 (1970).
12. D. G. Wickham and W. J. Croft, "Crystallographic and Magnetic Properties of Several Spinels Containing Trivalent Manganese," *J. Phy. Chem. Sol.*, 7 351–360 (1958).
13. S. Naka, M. Inagaki, and T. Tanaka, "On the Formation of Solid Solution in $Co_{3-x}Mn_xO_4$ System," *J. Mat. Sci.*, 7 441–444 (1972).
14. H. Bordeneuve, S. Guillemet-Fritsch, A. Rousset, S. Schuurman, and V. Poulain, "Structure and Electrical Properties of Single Phase Cobalt Manganese Oxide Spinels $Mn_{3-x}Co_xO_4$ Sintered Classically and by Spark Plasma Sintering (SPS)," *J. Sol. State Chem.*, 182 396–401 (2009).
15. H. Bordeneuve, A. Rousset, C. Tenailleau, and S. Guillemet-Fritsch, "Cation Distribution in Manganese Cobaltite Spinels $Co_{3-x}Mn_xO_4$ ($0 \leq x \leq 1$) Determined by Thermal Analysis," *J. Therm. Anal. Calorim.*, 101 137–142 (2010).
16. H. Bordeneuve, C. Tenailleau, S. Guillemet-Fritsch, R. Smith, E. Suard, and A. Rousset, "Structural Variations and Cation Distributions in $Co_{3-x}Mn_xO_4$ ($0 \leq x \leq 3$) Dense Ceramics Using Neutron Diffraction Data," *Sol. State Sci.*, 12 379–386 (2010).
17. M. Brieu, J. J. Couderc, A. Rousset, and R. Legros, "TEM Characterization of Nickel and Nickel-Cobalt Manganite Ceramics," *J. Eur. Ceram. Soc.*, 11 171–177 (1993).
18. Y. Zhu, J. Tafto, H. L. Bhaskar, and K. C. Nagpal, "Defects in High-Tc Cuprate Superconductors," *Mater. Res. Bull.*, 16 54–59 (1991).
19. R. Metz, R. Legros, A. Rousset, J. P. Caffin, A. Loubière, and A. Bui, "The NTC Thermistors of Low Resistivity of Low Resistivity and Large Stability," *Silicates Industr.*, 3 71–76 (1990).
20. S. Guillemet-Fritsch, *et al.* "Structure, Thermal Stability and Electrical Properties of Zinc Manganites," *Sol. State Ionics*, 128 233–242 (2000).
21. A. D. Daguar Broemme, "Physico-Chemical Investigations on Co-Mn Oxide Spinels", Thesis, Eindhoven University of Technology, Eindhoven, The Netherlands, 1990.
22. S. Sakamoto, M. Yoshinaka, K. Hirota, and O. Yamaguchi, "Fabrication, Mechanical Properties, and Electrical Conductivity of $Co_3O_4$ Ceramics," *J. Am. Ceram. Soc.*, 80 267–268 (1997).

23. P. A. Cox, *The Electronic Structure and Chemistry of Solids*, Oxford Science Publications Edition, New York, 1987.
24. A. Rousset, A. Lagrange, M. Brieu, J. J. Couderc, and R. Legros, "Influence of the Microstructure on Electrical Stability of NTC Thermistors," *J. Phys. III Fr.*, 3 833–845 (1993).
25. B. Gillot, J. L. Baudour, F. Bourée, R. Metz, R. Legros, and A. Rousset, "Ionic Configuration and Cation Distribution in Cubic Nickel Manganite Spinels $Ni_xMn_{3-x}O_4$ in Relation with Thermal Histories," *Sol. State Ionics*, 58 155–161 (1992).
26. E. Elbadraoui, *et al.* "Cation Distribution, Short-Range Order and Small Polaron Hopping Conduction in Nickel Manganites, from a Neutron Diffraction Study," *Phys. Stat. Sol. (b)*, 212 129–139 (1999).
27. E. Elbadraoui, J. L. Baudour, F. Bouree, B. Gillot, S. Fritsch, and A. Rousset, "Cation Distribution and Mechanism of Electrical Conduction in Nickel-Copper Manganite Spinels," *Sol. State Ionics*, 93 219–225 (1997).
28. A. Rousset, R. Legros, and A. Lagrange, "Recent Progress in the Fabrication of Ceramic Negative Temperature Coefficient," *J. Eur. Ceram. Soc.*, 13 185–195 (1994).
29. S. T. Kshirsagar and C. D. Sabane, "Electrical Conduction of Tetragonally Distorted Manganites Spinels. Jap," *J. Appl. Phys.*, 10 794–802 (1971).
30. E. Jabry, A. Rousset, and X. Lagrange, "Preparation and Characterization of Manganese and Cobalt Based Semiconducting Ceramics. A.," *Phase Transit.*, 13 63–70 (1988).
31. H. St O'Neil, "Thermodynamics of $Co_3O_4$: A Possible Electron Unpairing Transition in $Co^{3+}$," *Phys. Chem. Miner.*, 12 149–154 (1985).